Turk J Elec Eng & Comp Sci, Vol.18, No.3, 2010, © TÜBİTAK
doi:10.3906/elk-0912-15

Dual-use of compact HF radars for the detection of mid- and large-size vessels

Hugh J. ROARTY[1], Don E. BARRICK[2], Josh T. KOHUT[1], Scott M. GLENN[1]
[1] *The Coastal Ocean Observation Laboratory, Institute of Marine and Coastal Sciences Rutgers, The State University of New Jersey, New Brunswick, NJ 08901 USA*
e-mail: hroarty@marine.rutgers.edu
[2] *CODAR Ocean Sensors, Ltd., 1914 Plymouth Street Mountain View, CA 94043 USA*

Abstract

This paper describes the development of the SeaSonde High Frequency Radar system into a dual-use application for the mapping of ocean surface currents and detection of ships at sea. This development entailed the creation of a new radar waveform that would permit this dual-use as well as a detection algorithm to identify the ships in the radar spectra. The detection algorithm utilizes two methods for calculating a background signal level: an infinite impulse response (IIR) filter and a two-dimensional median filter. These two methods are employed simultaneously with multiple length averaging times to maximize the number of detections. The initial phase of development focused on improving the radar waveform to maximize the results for ship detection while still retaining the ability to measure surface currents. The latter phase of the development concentrated on testing the detection algorithm on a known vessel in different environmental conditions.

Key Words: *HF radar, object detection, networks, ocean currents, remote sensing.*

1. Introduction

High Frequency Surface Wave Radars (HFSWRs) are proliferating as backbone instrumentation within the United States Integrated Ocean Observing System (IOOS). The main purpose of these radars is for environmental mapping of sea conditions such as surface currents, sea state and wind direction [1]. Figure 1 shows a recent map of ocean surface currents off the eastern United States from Cape Cod to Cape Hatteras. This map was created from the radial vectors generated by thirteen long-range (5 MHz) HFSWRs. The inset of Figure 1 shows wave height, period and direction data from one of those radars. However, another application for these radars is for the detection of vessels at sea [2]. Typical ship velocities fall in the same span as the Bragg waves from which currents and waves are derived. Echoes from ships are therefore frequently seen, and are considered clutter in the processing of sea echo to measure sea conditions. However, radar signal and processing parameters for measuring surface currents do not always match the best settings for detection of hard targets. Different

signal transmission and processing options were tested to determine the optimal settings for a dual-use radar (simultaneous current mapping and vessel detection). With these "optimal" settings, the radars collected echo time series vs. range data. These range data were processed into Doppler spectra using multiple-length fast Fourier transforms (FFTs) developed for this application. The Doppler spectral data were then run through a detection algorithm to pick out the vessel targets.

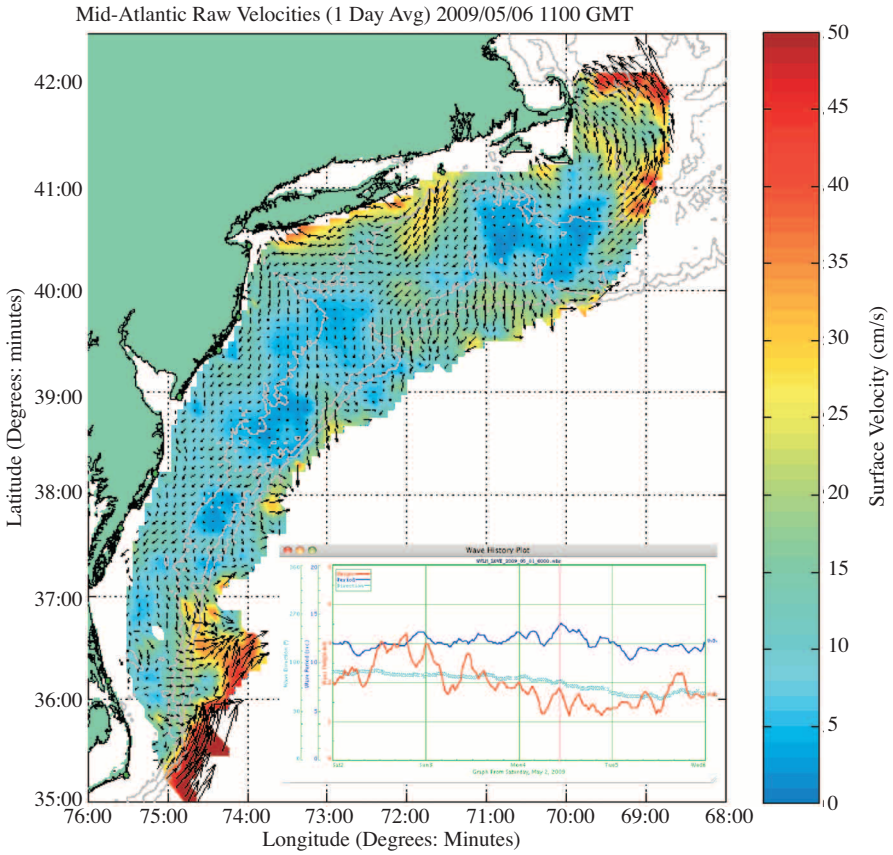

Figure 1. Map of surface currents from Mid Atlantic High Frequency Radar Systems. There are a total of 27 HF radars in the Mid Atlantic that are operational for environmental monitoring. The speed of the currents are displayed from the color bar on the right with the arrows indicating direction. Wave height (red), period (blue) and direction (aqua) from one of the radar systems is shown in the inset.

The detection algorithm consists of:

1. Calculating a background level of the Doppler spectrum by two different methods
2. Setting a threshold (typically 6-9 dB) above the background
3. Any signal above the threshold is considered a detection—the classic Constant False Alarm Rate (CFAR) detection algorithm.

A Global Positioning System (GPS) track record from the vessel was used as ground truth for the potential detections and served to optimize the algorithms.

2. A different approach—network coverage and multi-statics

This section introduces and discusses a departure of our approach from conventional radar ship surveillance—both High Frequency (HF) and microwave. HFSWRs [3] and sky wave radars ..[4] have been utilized for the detection of ships at sea. In the conventional approach, a single radar operates as a stand-alone system. Transmitter and receiver are collocated, and the radar is called backscatter or monostatic. If a target is successfully detected above the background, its position is given in polar coordinates, i.e., range and bearing from the radar. At HF, these single backscatter systems have weaknesses. Because target Doppler measurement is an accurate and critical HF observable, the vessel must compete with sea clutter, whose speed-induced Doppler causes it to fall in same velocity span as the targets being detected. The dominant sea echo is the first-order Bragg scatter that comes from ocean waves of half the radar wavelength; this echo is generally larger than the echo from even the largest supertanker. Surrounding the Bragg peaks are second-order sea echoes that lay 15 - 40 dB lower, but usually well above the background noise. Taken together, these sea echoes can mask and/or hinder detection of perhaps 40% of candidate ships. Sometimes a ship may be seen, but as it changes course or speed, it will enter a region of high sea clutter and disappear from radar view. As a countermeasure, it is trivial for a ship navigator to determine the frequency of the HF radar, and in order to evade detection, adjust speed/course so that it will be masked by the strong sea-clutter spectral background. Conceptually, if the radar could change operating frequency by a significant increment (e.g., factor of two), a ship hidden by a Bragg peak would be unmasked. Such complexity drives up the cost of the radar significantly.

The build-up of coastal HF radar networks in the U.S. and elsewhere for IOOS-related current and wave monitoring offers an opportunity to conceive of a different approach to ship surveillance with the conventional single backscatter radar scenario described above. The backscatter radars of these distributed networks are spaced sufficiently close together that the same spot on the sea is observed by at least two radars. When applied to ship detection, this means that the same vessel will be viewed from two or more different angles leading to several advantages. First, in the distributed network if the target's radial velocity with respect to one radar is masked by a sea-echo spectral peak, a second radar or a third—seeing a different radial velocity from that target—will uncover the target. Second, if the transmitter of one radar (or a transmitter on a buoy) serves as the target illuminator, then the echo seen by a second receiver (the multi-static configuration) cannot also be masked. In other words, different simultaneous observing geometries have the advantage of unmasking a target hidden in the clutter of a single radar. Third, external noise bursts—that can cause loss of detection at one radar receiver—rarely occur at the same range/Doppler for two or more radar receivers. Fourth, even if the masking is not a problem, multiple solid observations of the same target increase the probability of detection and reduce false alarm rate.

Multiple observations of the same target entail another algorithmic function that must be added to the detection-tracking process. This function is the association task: which detection seen by one radar observation is the same as one seen by another radar? Or, is one seeing a new target that is close to the first? The development of this association algorithm can also aid in target identification / classification. It improves the tracking accuracy significantly: bearing accuracy, which is the weakest observable at HF, is mitigated by the triangulation offered by multiple observations of the same target. In addition, it can feed back information to the detection process of radars that may have lost the target as it moved into sea-echo peaks: i.e., one radar can inform another radar where to look for the target as it emerges from the sea clutter. We will examine the

ramifications of this multi-observation system enabled by the network approach to HF radar configuration that is being put into place for other purposes.

3. Network operation and data collection

The HFSWR used for these experiments was the SeaSonde developed by CODAR Ocean Sensors. The SeaSonde has been in use for the past two decades for the mapping of ocean surface currents [5]. This paper explores the dual-use aspect of the SeaSonde for measuring surface currents as well as detection of hard targets (ships). Signals from ships were seen in the data from the outset of the development process for current and wave monitoring. Since the SeaSonde was designed to extract information from the sea echo, algorithms were developed to remove the ship echo from the data. The algorithms that have been specifically developed to extract the ship information from the data will be explained later.

The SeaSonde is capable of operating monostatically, where the transmit and receive antennas are collocated, as well as bistatically, where the recorded signal originates from a transmitter some distance from the location of the receiver. The radars are capable of operating bistatically by using GPS synchronization timing [6]. A network of radars is then capable of operating multi-statically where the individual radars are observing simultaneously in monostatic and several bistatic modes. The Rutgers HF Radar Network was operated multi-statically for the tests discussed here.

The first pair of these radars was installed at Brigantine and Brant Beach, NJ in 1998, followed in 2000 by long-range versions at Loveladies, Wildwood, Sandy Hook, and Tuckerton, NJ. A map showing the location of the four long-range SeaSonde units is shown in Figure 2a. Each radar site consists of a Codar SeaSonde system housed in a climate controlled enclosure with cables leading to the transmitter and receiver antennas typically deployed on the beach near the dune line. Figure 2b shows the radial vector density for 2003, the second year of the study. The radial vectors from each site were produced every three hours. The long-range transmit antenna is a monopole with height of a quarter wave length (15 m) of the transmitted signal, nominally 5 MHz. The receive antenna consists of an omnidirectional monopole and two directional crossed loops [7], [8]. A picture of one of the compact radar installations is shown in Figure 3. The spacing between the antennas is approximately one wavelength, 60 m in this case for a 5 MHz system. The radars have been in constant operation since their installation.

The SeaSonde is a direction-finding HF radar system. A direction finding system measures the returned signal over all directions on the three receive antennas. These signals are then passed through the multiple signal classification (MUSIC) algorithm to determine bearing of the incoming signal [9].

The antenna pattern is a measure of the response of each element to incoming signals. The ideal loop pattern free of any distortion is a sinusoid; two crossed loops have a sine and cosine pattern over bearing angle. When the antenna is placed in the field, objects in the near field (within one wave length) can couple with the antenna and distort the ideal pattern. That is why it is important to always measure the antenna pattern when the system is first installed to quantify and correct for any possible distortion [10]. Any distortion will impact the bearing determination of the incoming signal. The antenna patterns of all systems were measured and used by the detection algorithm.

The nature of the vessel tracking tests varied in the initial stages. Vessel detection tests used multiple ships (dedicated vessels as well as ships of opportunity), of various sizes, to test different signal transmis-

sion/processing options, in order to optimize the SeaSondes for dual use (simultaneous current mapping and vessel detection). Examples of associated GPS tracks for each test are plotted as the aqua lines in Figure 2A. At the conclusion of this initial set of tests, the Rutgers network was modified based on lessons learned in Year 1. The best dual-use waveform, which will be explained later, was installed on all systems. GPS timing was adjusted for multi-static data collection from all four New Jersey long-range sites. Data archiving was done for range files, which are a collection of consecutive time sweeps consisting of received signal power versus range. The data processing paths for ship detection and current mapping diverge after the range file creation. Archiving these

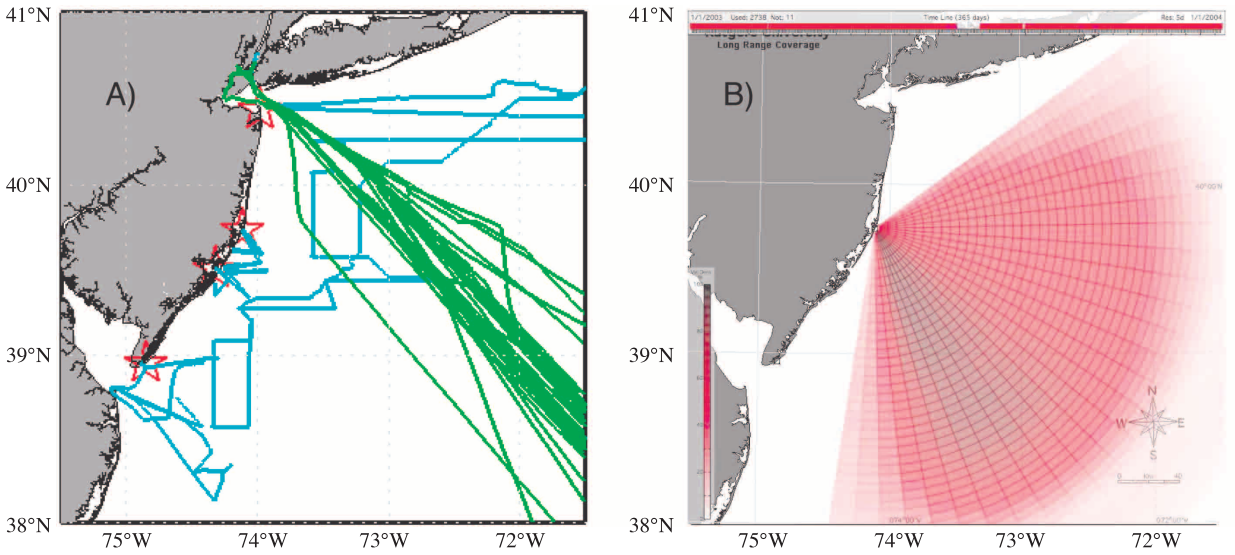

Figure 2. (A) Study area off the coast of New Jersey showing the location of the four long-range SeaSonde units as red stars. The tracks of the vessels in year 1 (aqua) and year 2(green) used for the study. (B) The radial vector density from the Loveladies SeaSonde site for year 2. The polar grid delineates the angular and range bins of the radar. The color bar is on the lower left hand side to illustrate spatial coverage and the timeline along the top shows temporal coverage.

Figure 3. Picture of 5 MHz long-range SeaSonde. The receive antenna is shown in the foreground on the right. The transmit antenna is shown in the background on the left. Technicians installing the radar are shown for scale.

range files enables use of multiple-length FFT post-processing for vessel tracking that was not necessary for current mapping. The radar sites were able to measure currents during this entire time period [11] when the ship detection capability of the radar was being developed.

A long-term test of the multi-static network was begun using a single known ship, the M.V. Oleander ..[12], as a known, reliable test target that could be examined under a variety of environmental conditions. The Oleander is a container ship that maintains a weekly schedule of transits between New York and Bermuda. GPS tracks obtained from the University of Rhode Island (green lines in Figure 2A) indicate that the Oleander usually approaches and departs New York Harbor along the Hudson Canyon traffic lane and only once used the north-south Barnegat traffic lane. Over 7 months of multi-static SeaSonde data at the range file level were collected and archived at the four long-range radars. The GPS data were used to identify times when the Oleander was within 200 km of Sandy Hook for detection processing.

4. HF radar target observables

HF radar ship (or hard target) detection and processing is much different from standard microwave radar target detection, because the HF radar signals and processing, including use of direction finding instead of beam scanning for bearing determination, are significantly different. The HF ship-detection observables listed in order of accuracy and importance are:

1) **Echo Doppler shift, and thence radial velocity**. This is the most accurate and meaningful parameter from an HF radar. It is usually nonexistent in conventional microwave target detection. The equation used to calculate radial velocity is given as

$$v_r = \frac{f_d \lambda}{2},$$

where v_r is the radial velocity (m/s), f_d is the Doppler frequency(s^{-1}), λ is the radar wave length (m). The sign convention here is positive for targets approaching the radar and negative for targets receding from the radar. The velocity resolution for the SeaSonde system operating at the nominal 5 MHz is 3 cm/s with a maximum velocity of 15 m/s before aliasing within the Doppler window for each range cell.

2) **Target range**. This is also quite precise, but is quantized based on the bin size (e.g., 1.5 km, 3 km or 6 km, depending on the signal bandwidth). The range to target for any radar depends on the time delay of the scattered signal after transmission. The SeaSonde employs a unique, patented method of determining the range from this time delay. By modulating the transmitted signal with a swept-frequency signal and demodulating it properly in the receiver, the time delay is converted to a large-scale frequency shift in the echo signal. The frequency shift is used to calculate distance to target. The detection algorithm does a fit to range bins in order to narrow the range more precisely. This fit uses a centroid calculation of the sum of the product of the signal range and power divided by the sum of the signal power. This range measurement is quite accurate, depending on the Signal to Noise ratio (SNR).

3) **Target bearing**. This is calculated for the echo at each spectral point (range and speed) by using simultaneous data collected from the three collocated directional receive antennas (two crossed loops and a monopole). The complex voltages from these three antennas are put through a 'direction-finding' (DF) algorithm to get the bearing. The particular, patented algorithm adapted and perfected for the SeaSonde is referred to

as MUSIC [13]. Bearing is the poorest observable, and is usually noisy. This is the nature of working with compact antennas designed for frequencies 1000 times lower than microwave. With microwave radars, range and bearing are quite accurate observables while range rate is not directly observed.

4) **Target echo amplitude** (from the signal strength). As with microwave radars, this echo amplitude is a fluctuating quantity, depending on ship aspect, sea state, and other environmental factors. Target amplitude can be used to calculate the target radar cross section (RCS). The RCS is a very good identifier of the nature of the target, i.e., its size and sometimes its shape.

5) **Uncertainties** in the first three quantities are calculated and included in the detection file for a suspected target. These are estimated based on resolution, SNR and other considerations.

5. Waveform

The SeaSonde is unique from most microwave radars in the fact that it does not use pulsing to determine range to the target. Range is determined by using a waveform with a repeating linear frequency sweep. However, unlike time-domain pulse compression used with chirp waveforms for microwave radars, the echo time delay shows up as a frequency offset between the presently transmitted signal and the received target signal. Pulsing is used by the SeaSonde only so that the receiver and its incoming signal integrity will not be damaged nor limited by swallowing an intense transmit signal while receiving the weaker target echoes. Thus, we consider the pulsing only as a means for turning the transmitter and receiver on and off at complementary times, to preserve this integrity. In the case where transmitter and receiver are separated (called a bistatic radar), pulsing is not necessary and not used by the SeaSonde, because the separation between the two prevents damage to receiver and signal integrity.

The signal-to-noise ratio, SNR, in any optimized receiver (referred to as a "matched-filter receiver") is proportional to the average power, not the peak power. By pulsing, for a given maximum peak power, the average power—and hence the SNR—is reduced. If one must pulse so that transmitter and receiver are not on at the same time, the best one can do in maximizing average power is a 50% duty-factor signal. This happens when the receiver/transmit on/off patterns are identical. The simplest way to do this is a square wave. All SeaSonde waveforms were invented to employ this maximum 50% duty factor pulsed waveform, but to do so in a manner that optimizes the SNR over the coverage region of interest [14]. In addition, the square-wave edges of the transmit signal are tapered slightly. This goes a long way to reducing spectral harmonics of the pulsing that cause slower roll-off of the signal away from the edges of the sweep, thereby mitigating interference possibilities to others. The pulse tapering that was used reduces the duty factor only slightly, i.e., to about 48%.

For current mapping from the sea echo, pulsing/gating has another advantage. Sea echo is a strong signal that appears in every range cell. Echoes, however, fall off very rapidly with distance from the radar. Hence, strong echoes in early range cells must be suppressed so their range-processing side lobes don't overwhelm the weaker echoes further out, mitigating this dynamic range constraint. This is achieved for microwave radars by using sensitivity-time control circuitry. Square wave pulsing meets this requirement by reducing echoes from early range cells at no expense to weak echoes from distant ones.

All standard SeaSonde systems are designed to operate optimally for sea echo, i.e., current mapping. However this waveform is not optimal for detection of smaller vessels in close range cells. It was the aim of the research done here to optimize the radar wave form for both current mapping as well as target detection. This entails optimizing the waveform to identify small targets closer to the radar where their echo SNR is much

weaker than that of the sea echo, rendering the signals too weak to be detected. This waveform was designed to increase the SNR of signals close to the radar while not compromising the SNR at distant ranges from the radar. To illustrate this design progression see Figure 4 which details three types of square wave pulsing with different lengths. The longer curve shown in red has a pulse length optimized for measuring surface currents using the 5 MHz long-range SeaSonde, about 2000 microseconds long. Two other pulsing options are shown in the middle panels. The one on the left uses mixed length pulsing and is used for calibrating the radar. The one on the right is a combination of the one optimized for currents and the one used for calibration which is given the name enhanced. The waveform duty factors for the three wave forms are shown and compared in the bottom panels. The duty factor is the fraction of signal that is available for use in the detection process. In the case of the wave form designed for currents measurements (red), 100% (0 dB) of the signal scattered off a target (waves or ships) at a range 190 km are available for reception at the receiver. Whereas, the signal scattered off a target at a range of 10 km is only visible to the receiver 0.1% (-30 dB) of the time. When the pulse is scattering off these close targets the receiver is off most of the time. Only at the end of the pulse does the receiver turn on and is able to receive signals from close targets. The receiver is on the entire time and is able to receive the full scattering signal from targets at a range of 190 km.

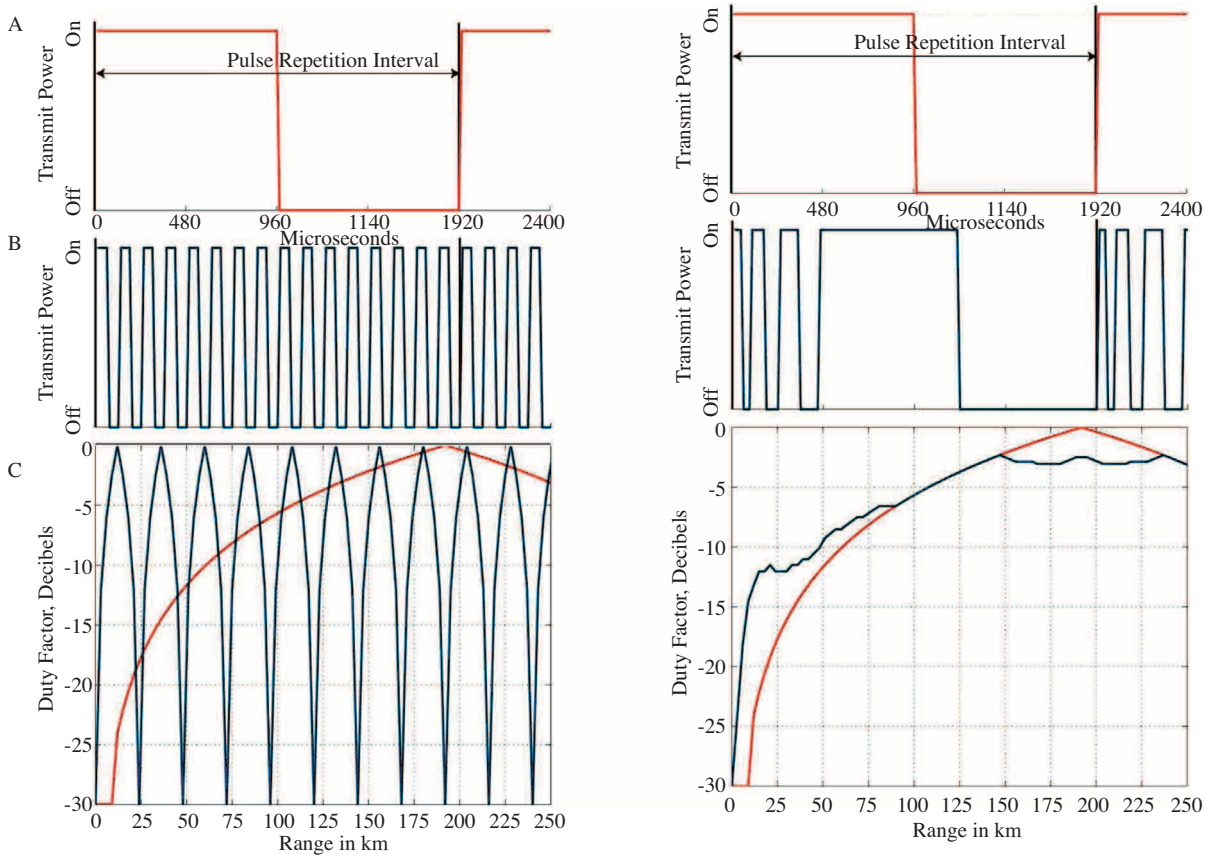

Figure 4. (A) Square-wave pulsing (red line) suitable for long-range current mapping. (B) Mixed length pulsing (left) used for calibration measurements of the radar. Enhanced pulsing (right) increases signal strength on targets close in, while minimizing loss at greatest range. (C) Duty factor vs. range for the three pulsed waveforms, square (red), mixed (blue, left) and enhanced (blue, right).

Figure 4 shows the standard square-wave pulsing installed on any standard Long-Range SeaSonde systems for current mapping, as the red upper curve. Its duty factor for target echo strength maximizes near 200 km, as shown in the lower panel. The blue curve in the middle left represents a very short-pulsed square waves that has been used for antenna pattern calibrations. This simple waveform offers much greater echo power close in, out to $\sim$11 km; it can be greater by nearly 30 dB from the long-pulse red duty factor, seen from the lower panel. However, it has blind zones at 25 km, 50 km, etc.

The waveform shown in Figure 4 on the middle right shows the compromise developed for dual use. Here, a 50% duty factor is achieved, the best that can be done. At close in ranges, power is higher by 13 dB from that of the default long square wave (compare the difference between red and blue curves in the lower panel at 25 km). On the other hand, there are no blind zones in the coverage area. Furthermore, the power at maximum range (200 km) is only down by 2.5 dB. This waveform was set at the beginning of Year 2 and is currently being used on all Rutgers long-range SeaSonde systems. In addition to being beneficial for hard target detection this wave form is also useful in increasing weaker close-in signals from the second-order sea echo which are utilized for wave parameter (height, period, direction) estimates.

6. Ship detection algorithm

The ship detection algorithm uses a straightforward thresholding scheme, which is known in the microwave radar community as constant false alarm rate CFAR. After a peak (local maximum) in the spectral domain (range-Doppler space) is identified, its SNR, which is the signal power divided by the noise floor or background power, has to be above a preset threshold for antenna 3 (monopole) and at least one of the two loops (antenna 1 or 2). Usually a threshold of six to ten dB gives good detection rates at HF without too many false positives. The thresholding is excluded for regions around the zero-Doppler position and sea-echo Bragg peaks. Both regions produce strong signal returns that would make detecting a ship nearby very difficult. The zero-Doppler is from signals returned from any stationary object wile the sea-echo Bragg peaks are due to signal returns off ocean waves with half the wavelength of the transmitted radio signal [15]. Currently two bins on each side of zero Doppler and Bragg peaks are excluded.

Two types of background calculations were used to identify the noise floor: a 2-D median filter that averages by finding the median in Doppler space and range, which was based upon an image processing algorithm [16], and an Infinite Impulse Response (IIR) filter that averages in time, also known as an exponential smoother [17]. An example of the two background calculations is shown in Figure 5. Panel 5A shows the power spectrum with the IIR background. Panel 5B shows the power spectrum and the median background. The peak that represents a ship (marked by the arrow) can be identified above the background plus threshold in both cases. The two backgrounds produce a different SNR for this vessel, 15.0 dB for the IIR background and 11.3 dB for the median background. Note that the zero-Doppler and Bragg peaks in the IIR background are thicker due to lower resolution. Hence the median background has the potential to detect targets closer to these regions. The pros and cons of the two methods are discussed in Table 1.

Since these two methods complement each other, it was decided that the best strategy is to employ both at the same time. Also built into the detection algorithm is the ability to use simultaneous different-length, multiple sliding window FFTs in the Doppler processing. Typical FFT lengths range from 8 to 1024 points.

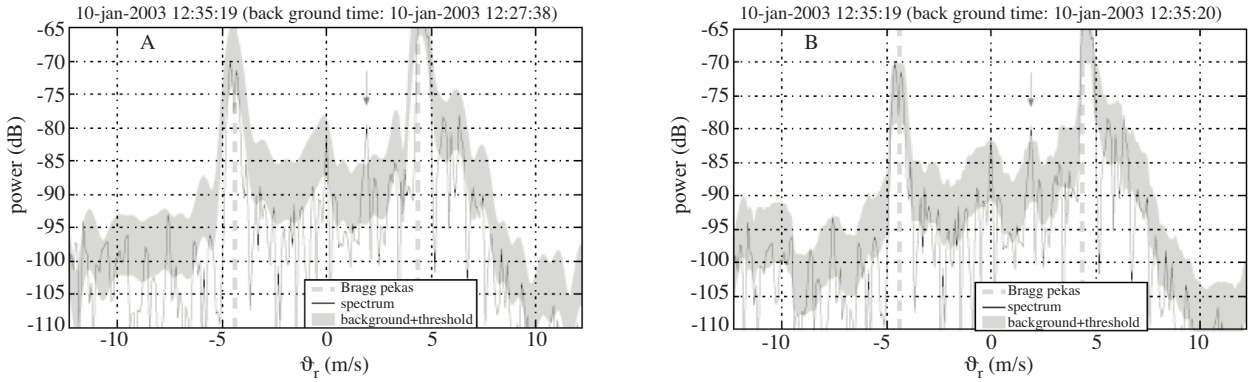

Figure 5. Power spectrum compared with two types of background (a) Infinite Impulse Response and (b) Median. The FFT length is 256 and the IIR background length is 64. The threshold is 7 dB for both. The ship is marked by the arrow between zero Doppler and 5 m/s radial velocity.

Table 1. Pros and Cons of IIR Background versus median background.

	IIR Background	Median Background
Pros	• Fast for multiple FFTs • Smoother variation in time • More consistent results during calm ocean	• Fast for short FFTs • Faster response • Possible detection closer to zero-Doppler and Bragg peaks
Cons	• Have to wait for onset of detection (edge effect) • Slower response time • More prone to false positives during times of interference	• Slower for multiple FFTs • Less consistent tracks during calm ocean • Detection at edge range bins less reliable

7. Test results

One case study is presented here to display the current capability of the detection system. This example is for the transit of the vessel Oleander out of New York Harbor on February 21, 2004. The center transmit frequency of the radar was set to 4.55 MHz with a bandwidth of 25 kHz, which results in a range cell size of 5.85 km. The range data from the radar was passed onto the detection algorithm. The detection algorithm was run using six parallel processes: three using the median background with 64, 128 and 256 point FFTs and three using the IIR background with 128, 256 and 512 point FFTs. All six processes used a 32 second update interval. The Oleander became visible to the radar at approximately 0030 GMT and was 150 km from the radar at 0600 GMT. The thresholds that were used with each FFT length are given in Table 2. The threshold used in the SeaSonde processing for currents is 6 dB, so that was used as the starting point. The threshold was increased

by 1 dB for each doubling of the FFT length because it was learned through previous runs of the algorithm that the average SNR increased by 1 dB with each doubling of the FFT. This trend is generally expected as the SNR should increase by 3 dB for a constant Doppler target when doubling the FFT length. The fact that average SNR only increased by 1 dB reveals the inconsistency of the target velocity/Doppler over the time intervals. The matrix shown in Table 2 is only one of several possible permutations for the FFT length and threshold level. The authors will explore the optimal settings in different environmental conditions for future work.

Table 2. Parameters used for one execution of the detection algorithm.

Nfft	Threshold Using Median Background (dB)	Threshold Using IIR Background (dB)
64	6	NA
128	7	6
256	8	7
512	NA	8

An example of the file output from the detection algorithm is shown as Table 3. This is the output using the median background with an FFT length of 512 points and a threshold of 8 dB. Each line represents one detection by the radar at one instance in time. The metadata is shown at the top of the file, preceded by percent symbols so they will be considered comments by programs that would be used to read the data. The columns of data reading from left to right for each detection are range cell number, Doppler velocity in spectral bins from the center, range (km), range uncertainty (km), radial velocity (m/s), radial velocity uncertainty (m/s), bearing of the target in degrees clockwise from north (° CWN), bearing uncertainty (°), longitude (°), latitude (°),east distance from the radar (km), north distance from the radar (km), signal to nose ratio for loops 1, 2 and 3 (dB), spectral power of the monopole (dB) and the radar cross section of the target (dB). A detection file is generated at every update interval.

A plot of all the detection files using the median filter with an FFT length of 256/8 dB threshold is shown in Figure 6. There are five other plots like this one corresponding to the five other detection methods, but they are not shown here to conserve space. The top panel shows detected points in range as a function of time over a four hour period. The second panel is the detected-peak Doppler shift, converted to range rate. The two yellow lines are the position of the Bragg sea echo. These regions constitute intense clutter peaks at and near which ship detection is difficult. Lastly, the bottom panel shows the bearing of the detected points. The solid yellow regions are bearing sectors over which it was not expected for the radar to make measurements (i.e. in back of the radar on land). The solid aqua line in all three panels is the ground truth data of the Oleander as derived from the GPS record of the vessel.

This detection process identifies many signals that exceed the threshold of 8 dB that was set. These are all candidate ships. Some are real vessels and some are false alarms. When one plots these points in range, range rate, and bearing as a function of time, patterns quickly emerge. A real vessel becomes obvious, as one will see a continuous trail of concatenated points as time marches forward as seen in the top panel of Figure 6. Many other points appear only once at or near any position in 4D space (range, range rate, bearing, and time). These are false alarms. They may be due to random atmospheric noise (e.g., near and distant thunderstorms) or radio interference. When all of these detection candidate points are plotted, their unique appearance has given rise to the descriptive term “pepper plots.”

Table 3. Output of detection algorithm. The columns of data reading from left to right for each detection are range cell number, Doppler velocity in spectral bins from the center, range (km), range uncertainty (km), radial velocity (m/s), radial velocity uncertainty (m/s), bearing of the target in degrees clockwise from north (° CWN), bearing uncertainty (°), longitude (°), latitude (°), east distance from the radar (km), north distance from the radar (km), signal to nose ratio for loops 1, 2 and 3 (dB), spectral power of the monopole (dB) and the radar cross section of the target (dB).

%ship_detect ver. : 3.1
%Rx(SEAB): 73.9728 40.3617
%TransmitCenterFreqHz: 1.346000e+07
%TransmitBandwidthHz: -4.943848e+04
%TransmitSweepRateHz: 2.000000
%lobe1_bearing(deg CWN): 130
%use measured pattern
%azLimit(deg cwn): -50 305
%Possible Targets: 14
%SNRThreshold(dB): 8
%Nfft: 512
%Rmax(km): 103.037
%TimeStamp: 2009 2 26 0 15 21
%timeConstforIIRfilterSec: 1800
%NfftBckGnd: 128
%bck.gnd.time_sec_ago: 416
%bck.gnd.time: 2009 2 26 0 8 25
%bin sizes(km, m/s): 3.03049 0.0435016

%nr %(0-based)	nv (DC-ctr)	R (km)	sigR (km)	-Vr (m/s)	sigVr (m/s)	az(CWN) (deg)	sigAz (deg)	longi (deg)	latitude (deg)	x(E) (km)	y(N) (km)	snr1 (dB)	snr2 (dB)	snr3 (dB)	P3 (dB)	RCS (dBsm)
0	-142	2.08	1.05	-6.18	0.015	285	14.02	73.949	40.367	-2	0.54	8.2	2.98	9.21	-106.5	-8.3
0	-41	1.26	0.49	-1.78	0.007	63	6.58	73.986	40.367	1.12	0.57	9.47	18.95	15.79	-101.7	-8
0	-38	1.21	0.52	-1.65	0.007	56	6.94	73.985	40.368	1	0.67	6.88	19.67	15.33	-102	-8.8
2	103	6.07	1.08	4.5	0.015	68	14.42	74.039	40.382	5.63	2.27	8.51	11.17	8.97	-82.8	26
3	-41	8.13	0.07	-1.78	0.001	61	0.95	74.057	40.397	7.12	3.94	24.02	32.18	32.62	-82	30
5	57	14.86	1.04	2.48	0.015	52	13.87	74.111	40.444	11.73	9.14	7.28	9.85	9.31	-92.3	27.2
7	-168	22.23	0.84	-7.32	0.012	259	11.27	73.715	40.323	-21.81	-4.27	7.86	8.03	11.12	-107.5	18.1
8	-80	23.88	1.18	-3.49	0.017	10	15.81	74.022	40.573	4.16	23.51	5.96	9.01	8.17	-104.3	22.5
11	236	32.02	1.09	10.26	0.016	305	14.62	73.662	40.526	-26.3	18.32	10.3	3.07	8.85	-107.5	24.8
14	120	41.08	1.09	5.22	0.016	300	14.59	73.552	40.546	-35.68	20.46	10.55	-0.19	8.87	-105.4	34.8
15	-211	45.7	1.15	-9.17	0.016	-40	15.36	73.624	40.676	-29.52	34.95	9.47	-5.18	8.42	-107.4	37.7
15	-180	47.66	1.06	-7.83	0.015	-48	14.17	73.553	40.648	-35.57	31.81	9.52	-16.77	9.12	-108.6	38.6
19	207	56.01	1.16	8.99	0.017	294	15.45	73.367	40.565	-51.32	22.61	9.4	-2.05	8.37	-108.1	48.5
30	71	89.8	1.16	3.07	0.017	304	15.57	73.088	40.81	-74.95	49.84	9.14	-5.94	8.31	-108.8	66.1

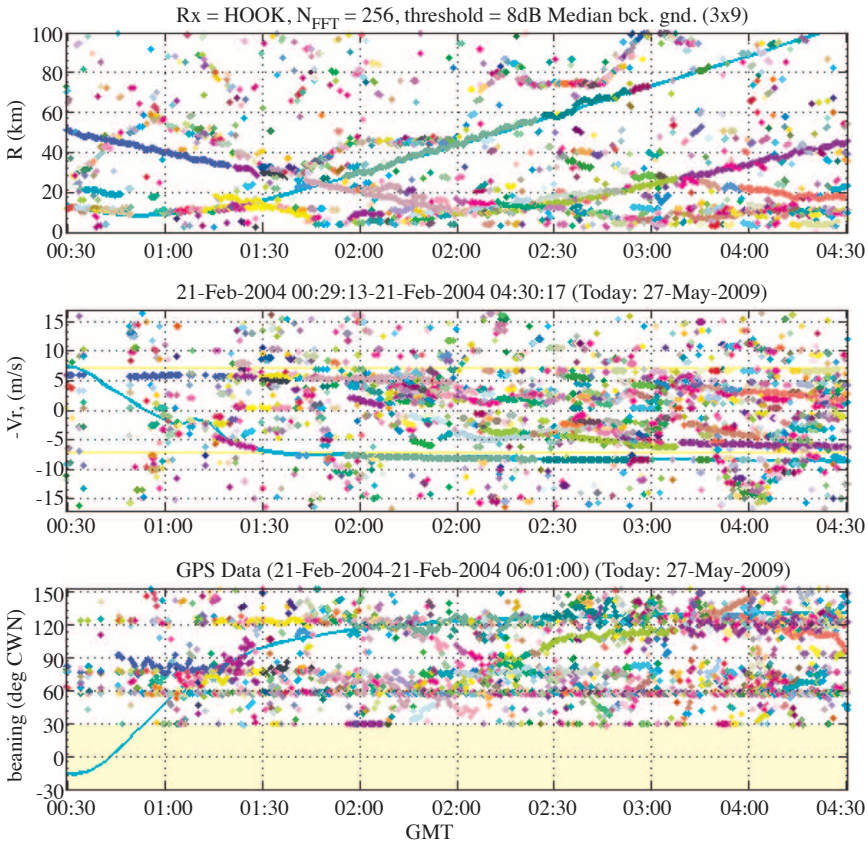

Figure 6. Detection results using the Median background with a 256 point FFT/8 dB threshold from the Sandy Hook radar site, February 21, 2004. The GPS track of the Oleander is shown as the solid aqua line. The algorithm is able to mark detections that are close in range or range rate with the same color.

Much of the volume of the pepper, i.e., point scatter, is controllable by the threshold that is set. The lower the threshold, the more pepper is admitted, becoming dominated by false alarms. The "false alarm rate" (FAR) is related to the threshold above the noise. For illustration we have included the results from another execution of the detection algorithm Figure 7. This shows the results of the detection algorithm using the Median filter with a threshold of 11 dB. Much of the pepper has been removed. The higher the threshold, the fewer false alarms, but then legitimate targets are missed (probability of detection, PD, goes down). FAR is exponentially (i.e., very strongly) related to threshold level, while PD varies much more slowly with threshold level. The philosophy we are exploring is that a higher FAR for dual-use HF radars is acceptable, because observation in 4D space and by multiple radars (overlapping backscatter and multi-static) will allow one to filter for the true ship target trails. This increases PD at lower SNR thresholds.

The valid detections on the Oleander for all six detection processes are shown in Figure 8. A detection is counted as valid when the calculated range is within half the width of a range bin and within two Doppler bins for speed. If the ship is seen by more than one detection scheme, the algorithm chooses the one with the largest SNR on the monopole. Figure 8 again shows range, range rate and bearing detections of the Oleander over a six hour period. The detections are represented by a square (error box) with half the height as on standard deviation and the width is the length of the FFT window. The solid aqua line in all three panels is the ground

truth data of the Oleander as derived from the GPS track record of the vessel. The six colors represent the six detection processes IIR-128 (blue), IIR-256 (red), IIR-256 (magenta), Median-64 (dark brown), Median-128 (brown), Median-256 (dark green). As the Oleander is departing NY Harbor and sailing past the Sandy Hook SeaSonde site, the radial velocity is changing. Over this section the shorter FFTs do a better job for the detections. As the Oleander reaches its cruising speed the longest FFT of the median background does the best for detecting the vessel. As noted in the radar observables the error bars for range and range rate are quite small while those for the bearing are the largest. The Oleander remained visible to the radar to a range of approximately 100 km and was seen 42% of the time. Including multiple length FFTs optimizes ship detection for the vessel type and velocity parameters: longer FFTs for larger vessels and shorter FFTs for smaller faster vessels. The advantages of calculating multiple length FFTs have been identified as a key design aspect of this detection scheme.

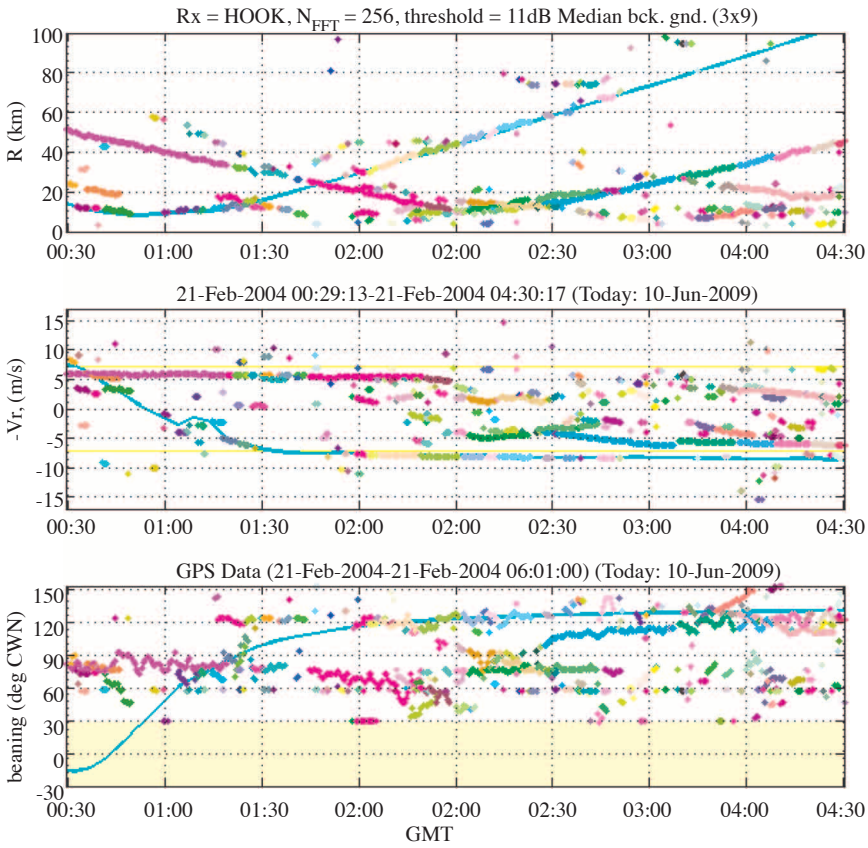

Figure 7. Detection results using the Median background with a 512 point FFT/11 dB threshold from the Sandy Hook radar site, February 21, 2004. The GPS track of the Oleander is shown as the solid aqua line. The algorithm is able to mark detections that are close in range or range rate with the same color.

8. Conclusions

As the number of HFSWRs for environmental monitoring increase, the potential exists to simultaneously use these instruments for detection of hard targets—a dual-use capability. This data stream can serve as an

additional layer for Maritime Domain Awareness (MDA). The radar waveform was modified from the form that was optimized for current measurements to one that will allow for a dual-use: mapping currents and detection of ships. The data stream was therefore split to generate two products, radial maps of currents and target files of possible detections. This proposed system is robust in that it can illuminate a single target from multiple sites monostatically, which were presented here, as well as bistatically, which will be presented in future work. This design prevents a vessel from hiding in the intense Bragg sea echo. The detection algorithm currently uses the GPS recorded on the vessel and/or the position information broadcast over the Automatic Identification System (AIS) to separate good detections from the false alarms. The AIS data will be utilized to refine the algorithm in a multi-ship environment. The authors also envision passing the detections onto an association and tracking algorithms to refine the position and filter out the false alarms.

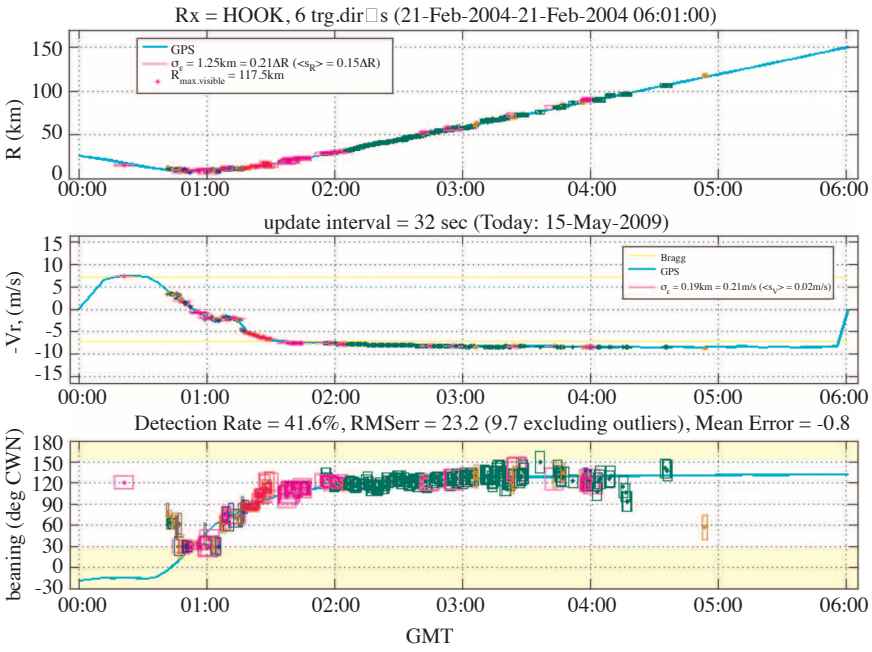

Figure 8. Valid detection results for all six processes of the Oleander from the Sandy Hook radar site, February 21, 2004. The error bars are for the six detection processes IIR-128 (blue), IIR-256 (red), IIR-256 (magenta), Median-64 (dark brown), Median-128 (brown), Median-256 (dark green).

Acknowledgements

This work was funded by the United States Office of Naval Research (N00014-02-10917), the United States Department of Homeland Security (N00014-06-1-0177) and the United States Department of Defense (NO 03-5412). The authors would like to acknowledge Dr. Bill Browning of Applied Mathematics, Inc. for his contribution to the detection algorithm development. The authors would also like to thank Erick Rivera Lemus for helpful comments and Igor Heifetz for help with figures.

References

[1] D.E. Barrick, J.M. Headrick, R.W. Bogle, D.D. Crombie, "Sea backscatter at HF: Interpretation and utilization of the echo", Proc. IEEE, Vol. 62(6): pp. 673-680, 1974.

[2] D.M. Fernandez, J.F. Vesecky, C.C. Teague, J.D. Paduan, K.E. Laws. "Ship detection with high-frequency phased-array and direction-finding radar systems", Geoscience and Remote Sensing Symposium Proceedings, 1998. IGARSS '98. 1998 IEEE International, 1998.

[3] R. Khan, B. Gamberg, D. Power, J. Walsh, B. Dawe, W. Pearson, D. Millan, "Target detection and tracking with a high frequency ground wave radar", Oceanic Engineering, IEEE Journal of, Vol. 19(4): pp. 540-548, 1994.

[4] J. Barnum,rShip detection with high-resolution HF skywave radar", Oceanic Engineering, IEEE Journal of, Vol. 11(2): pp. 196-209, 1986.

[5] J.D. Paduan, L.K. Rosenfeld, "Remotely sensed surface currents in Monterey Bay from shore-based HF-radar (CODAR)", Journal of Geophysical Research, Vol. 101: pp. 20669-20686, 1996.

[6] D.E. Barrick, P.M. Lilleboe, C.C. Teague, "Multi-station HF FMCW radar frequency sharing with GPS time modulation multiplexing", U.S. Patent SN 10/109,769.

[7] B.J. Lipa, D.E. Barrick, "Least-squares methods for the extraction of surface currents from CODAR cross-loop data: application at ARSLOE", IEEE Journal of Oceanic Engineering, Vol. OE-8: pp. 226-253, 1983.

[8] D.E. Barrick, B.J. Lipa, "Comparison of direction-finding and beam-forming in hf radar ocean surface current mapping", Phase 1 SBIR final report, Contract No. 50-DKNA-5-00092, 1996.

[9] D.E. Barrick, B.J. Lipa, "Radar angle determination with MUSIC direction finding", U.S. Patent 5,990,834.

[10] J.T. Kohut, S.M. Glenn, "Improving HF Radar Surface Current Measurements with Measured Antenna Beam Patterns", Vol. 20(9): pp. 1303-1316, 2003.

[11] D. Gong, J.T. Kohut, S.M. Glenn, "Seasonal Climatology of Wind-Driven Circulation on the New Jersey Shelf", Journal of Geophysical Research, Vol., 2009.

[12] T. Rossby, E. Gottlieb, "The Oleander Project: Monitoring the variability of the Gulf Stream and adjacent waters between New Jersey and Bermuda." Bulletin of American Meteorology Society, Vol. 79: pp. 5-18, 1998.

[13] R.O. Schmidt, "Multiple Emitter Location and Signal Parameter Estimation", IEEE Trans. Antennas Propaga, Vol. AP-34: pp. 276-280, 1986.

[14] D.E. Barrick, Belinda J. Lipa, P.M. Lilleboe, J. Isaacson, "Gated FMCW DF Radar and signal processing for range/Doppler/angle determination", U.S. Patent 5,361,072.

[15] D.D. Crombie, "Doppler spectrum of sea echo at 13.56 Mc./s", Nature, Vol. 175: pp. 681-682, 1955.

[16] M.A. Sid-Ahmed, Image Processing: Theory, Algorithms and Architectures: McGraw Hill. 1994.

[17] S.J. Orfanidis, Introduction to Signal Processing. 4th ed: Prentice-Hall. 1996.